Theoretical study of graphene nanoribbon field-effect transistors

Gengchiau Liang[1], Neophytos Neophytou[2], Mark S. Lundstrom[2] and Dmitri E. Nikonov[3]

[1]Deparrtment of Electrical and Computer Engineering,
National University of Singapore, Singapore, elelg@nus.edu.sg
[2]School of Electrical and Computer Engineering,
Purdue University, West Lafayette, Indiana 47907-1285
[3]Technology and Manufacturing Group, Intel Corp.,
SC1-05, Santa Clara, California 95052

Abstract

Carbon nanoribbons (CNRs) have been recently experimentally and theoretically investigated for different device applications due to their unique electronic properties. In this work, we present a theoretical study of the electronic structure, e.g. bandgap and density of states, of armchair carbon nanoribbons, using both, simple analytical solutions and numerical solutions based on a π-orbital tight-binding approach. Compared to carbon nanotubes (CNTs), the bandgap and the density of states of CNRs are smaller, attributed to the different boundary conditions (rolled-up graphene vs. planar). The device performance of CNR MOSFETs can potentially outperform planar Si MOSFETs, and compete with high performance CNT MOSFETs.

Keywords: MOSFET, quantum confinement, carbon, graphite, current density, nanowire, ballistic transport

Introduction

Graphene sheet related materials are interesting for various fields due to their unique electronic properties. For example, two dimensional graphene sheets have been investigated for Quantum Hall effects [1], and carbon nanotubes (CNTs) have been widely studied for transistors [2], bio-sensors [3] and infrared emitters [4]. The CNT metal-oxide-semiconductor field-effect-transistor (MOSFET) has shown high performance, and is a possible candidate of a new channel digital logic switch. For realistic IC applications utilizing CNT MOSFETs, however, material properties such as the bandgap (E_G) have to be precisely controlled. Although the bandgap of a CNT is a strong function of its chirality [5], there is currently no straightforward way to control the CNT chirality during growth.

Recent studies on carbon nanoribbons show an alternative method to bypass the CNT chirality challenge and retain the excellent electronic properties of the graphene sheet such as light effective mass [6] and high electron/hole mobility [7], properties which appear in the CNTs. CNRs are graphene sheet monolayers edged along a specific channel direction with a narrow (few nanometers) channel width. Depending on the different orientations and widths, CNRs exhibit different electronic properties, similar to the dependence of CNTs on chirality. They can be metallic or semiconducting with the bandgap depending on their width [8]. Fig. 1(a) shows the atomic structure of armchair carbon nanoribbons which are one type of CNR configuration, and have semiconducting electronic properties; cf. Fig 1(b). The electronic structure is calculated using a simple π-orbital tight-binding approach. To investigate the ballistic performance of CNR MOSFETs (the device structure is shown in Fig. 2 (a)), the corresponding calculated bandstructure of the CNR, and the semi-classical "top-of-the-barrier" ballistic model [9, 10] are used. The simulated results show that the ON-current of a 1.4 nm wide, single gate CNR MOSFET under $V_{DD}=0.4$ V is approximately 1100 μA/μm, outperforming silicon MOSFETs in terms of drive current capabilities by over 80%. Compared to a 1.0 nm diameter CNT MOSFET whose circumference is around 3nm in a cylindrical geometry, cf., Fig. 2(b), the 1.4nm wide, single gate CNR MOSFET, however, shows much less ON current density under same the operation bias. To enhance the device performance of CNR MOSFETs, the double gate structure is employed. The double gate CNR MOSFET with 1.4 nm width has comparable performance to the CNT in terms of ON-current density. If a 3nm wide double gate CNR MOSFET whose width is closer to the circumference of the 1.0 nm diameter CNT is considered, it would outperform the 1.0 nm diameter cylindrical CNT MOSFET. Therefore, the results indicate that CNR MOSFETs can outperform Si MOSFETs and are comparable to CNT MOSFETs in terms of ON-current density capabilities.

Approach

To explore the fundamental electronic structure of CNR, the simple π-orbital nearest neighbor tight-binding model [5, 6, 8] is implemented. Our previous study has shown the dependence of orientation on electronic structures of CNRs. It was found that certain armchair MOSFETs are suitable

for MOSFET-like device applications due to their semiconducting properties and the absence of localized gap states [6]. Therefore, this study focuses on armchair CNRs. Their electronic properties are first investigated. Based on the simple approaches [9, 11] to obtain the relations between bandgap (E_G) and diameter (D) of CNTs, the relations between E_G and width of armchair CNRs (W) can be derived as following,

$$E_G(CNT) = \frac{0.8}{D}$$
$$E_G(CNR) = 0.8\,\frac{\pi}{2W} \qquad (1)$$

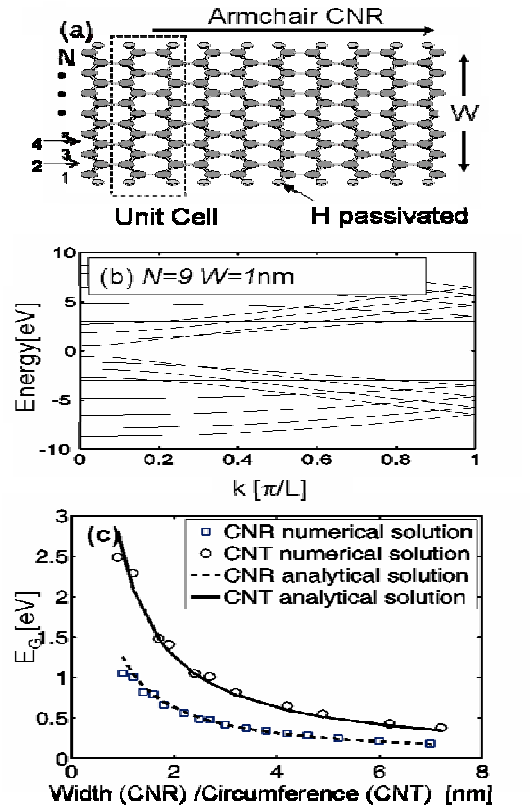

Figure 1: (a) Atomic structure of an armchair CNR. (b) Electronic structure of a 1nm wide armchair CNR calculated using simple π_z-orbital tight-binding approach. (c) Comparisons of Eg vs. Width for CNRs and Eg vs. circumference for CNTs for the simple analytical solutions and the numerical solutions.

Figure 1(c) shows the E_G vs. the width of the armchair CNRs and the E_G vs. the circumference of zigzag CNTs. Both results, the simple analytical solutions, and the numerical results of the tight-binding model are shown. A good agreement between these two different approaches is indicated. If the width of an armchair CNR is the same as the circumference of a zigzag CNT, the bandgap of the CNT is approximately twice than that of the CNR. It occurs because of the two different boundary conditions that the structures see. The CNT sees a periodic boundary (rapped-up graphene), while CNR sees a hard wall boundary (cut graphene). Quantum mechanically, these have significant role in the electronic properties of the materials. As a result, the valley degeneracy of the lowest subband of the zigzag CNTs is twice as that of the armchair CNRs. Accordingly, the density of states (*DOS*) of the lowest subband of zigzag CNTs, is twice as much as the *DOS* of the lowest subband of armchair CNRs'. The *DOS(E)* of the lowest subband of armchair CNRs' can be described as,

$$DOS_{CNR}(E) = \frac{1}{2} \times DOS_{CNT}(E)$$
$$= \frac{4}{3a|t|\pi} \times \frac{|E|}{\sqrt{E^2 - (E_G/2)^2}}\,\theta\left(E - E_G/2\right) \qquad (2)$$

where a is the bonding distance of carbon atoms in the graphene sheet, and $t=3eV$ is the hopping parameter used in this π-orbital tight-binding model. This information provides the physical insights of electronic structure of CNRs and CNTs, and helps in understanding their transport properties.

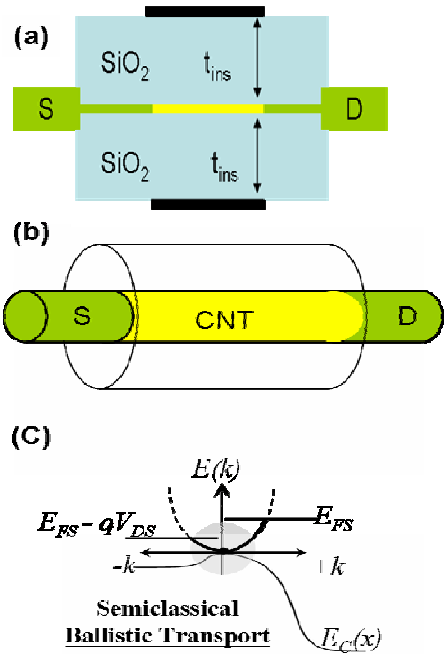

Figure 2: (a) and (b) schematic diagrams of a simulated double gate CNR MOSFET and a simulated surrounding gate CNT MOSFET. (c) The top-of-barrier ballistic MOSFET model. The charge on the top of the barrier and the ballistic current is calculated by the positive and negative going fluxes injected from the source and the drain, respectively.

To investigate the ballistic performance of CNR and CNT MOSFETs (device structure is shown in Fig. 2 (a) and 2 (b), respectively.), the semi-classical "top-of-the-barrier" ballistic model [9, 10] is employed with the corresponding calculated bandstructure. This model can capture 2D electrostatics based on a simple capacitance model, which is calibrated to the device structure. It also captures

NSTI-Nanotech 2007, www.nsti.org, ISBN 1420061828 Vol. 1, 2007

quantum capacitance through the self-consistent calculation. It calculates the carrier transport properties based on the electronic structure of the channel at the top-of-the barrier, cf., Fig. 2(c). Although it is a simple model, it provides insights of device physics and has been widely implemented in investigating the ultimate device performance of the different novel channel MOSFETs. The details regarding this model can be found in ref. [9] and [10].

Results and discussions

As shown in Figure 3(a), the ultimate performance of four different types of armchair CNR and zigzag CNT MOSFETs under V_G=V_{DD}=0.4 V is compared in terms of the total current they can carry. The I_D-V_{DS} characteristics of 1.4 nm wide armchair MOSFETs with a single gate (square) and a double gate (dash), a 1nm diameter zigzag CNT MOSFET with a surrounding gate (circle), and a 3.0 nm wide armchair CNR MOSFET with a double gate (solid), are presented. The 1.4 nm wide armchair CNR has a similar bandgap (~0.8eV) as the 1nm diameter zigzag CNT while the 3.0 nm wide armchair CNR has a similar width as circumference of the 1nm diameter zigzag CNT (its' circumference is around 3.1nm). In all of simulations the OFF-current density is set to 0.06 μA/μm and the oxide thickness to 1nm. The total current in the cases of the 1.4nm width armchair CNR MOSFETs is much smaller than the current carried by the 1.0nm diameter zigzag CNT MOSFETs. There are two reasons for this. First, as explained in a previous study [12], the degeneracy of the lowest subband of the zigzag CNT is 2, while that of the armchair CNR is 1. The *DOS(E)* of the former is twice as large as the *DOS(E)* of the latter, cf., Eq. (2). Therefore, the CNR MOSFETs provide less number of carriers during transport. This is true, however, if the total current through the devices is considered. The circumference of a 1nm diameter CNT, however, is larger than the width of a 1.4 nm width CNR. As the length of the conducting graphene increases, the number of carriers involved in transport increases. It is therefore, more appropriate to compare current density vs. V_D. As shown in Fig. 3(b), the current density shows different trends. The 1 nm diameter cylindrical CNT MOSFET still outperforms the 1.4nm width single gate armchair CNR MOSFET by 200% in terms of ON-current density. The 1.4nm width double gate armchair CNR MOSFET, however, has comparable performance to the 1 nm diameter cylindrical CNT MOSFET. Figure 4(a) explains the reasons behind this behavior. The mobile change density in the channel of the 1nm diameter CNT MOSFETs (circle) is much larger than that of the single gate 1.4nm width armchair CNR MOSFETs. Using a double gate geometry in order to increase the gate capacitance, however, makes the mobile change density in the CNR channel (dashed line) comparable to the mobile change density in the channel of the 1nm diameter CNT MOSFET. Although the injection velocity of the former is still a little less than the injection velocity of the latter as shown in Fig. 4(b), the overall current density is similar for these two types of devices. Therefore, upon comparing CNR and CNT devices, factors such as the gate geometry and the fact that a certain diameter CNT has a larger conducting circumference than a CNR of the same width should be taken into consideration.

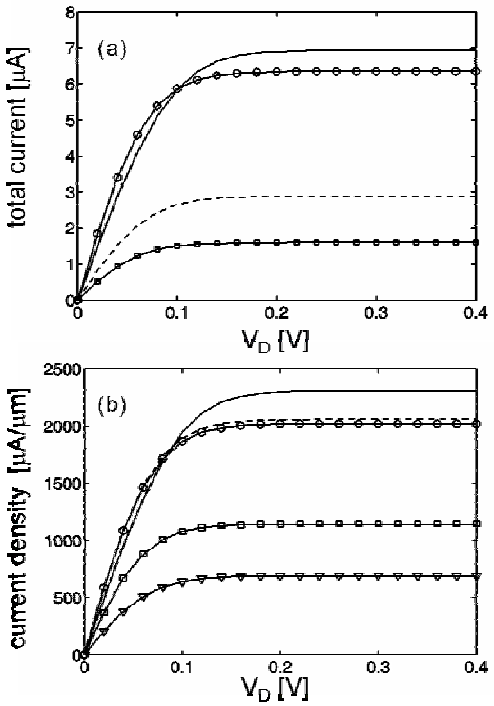

Figure 3: (a) I_D-V_{DS} characteristics of four types of MOSFETs at V_G=0.4V. These are a 1nm diameter CNT MOSFETs with the surrounding gate (circle), 1.4 nm width CNR MOSFETs with a single gate (square) and a double gate (dashed), and a 3 nm width CNR MOSFET with a double gate (solid). (b) Current–density vs. V_D at V_G=0.4 V for these four above devices and a single gate Si MOSFET.

Next, the ultimate performance of a 3nm width armchair CNR MOSFET with double gate structure is investigated in more detail. Comparing to the 1nm diameter zigzag CNT, the 3 nm wide armchair CNR has similar width as the circumference of the CNT, but has a smaller bandgap (~0.5 eV). As shown in Fig 3, comparing both quantities, (total current and current density), the double gate 3nm width armchair CNR MOSFET outperforms both the cylindrical 1nm diameter CNT MOSFET and the double gate 1.4nm width armchair CNR MOSFET. The reason for the better performance of the wider width CNR MOSFET has been explored in reference [6]. The effective mass of the wide CNR is lighter than the narrow CNR, indicating faster injection velocities. A similar study using a mobility model [7] also predicted that the wider CNR has larger carrier mobility. The higher velocity of this device is evident from

in Fig. 4(b). This is almost 50% larger than the second best (the 1nm CNT device), and overpasses its disadvantage of less mobile charge in the channel (30% less) as shown in Fig. 4(a).

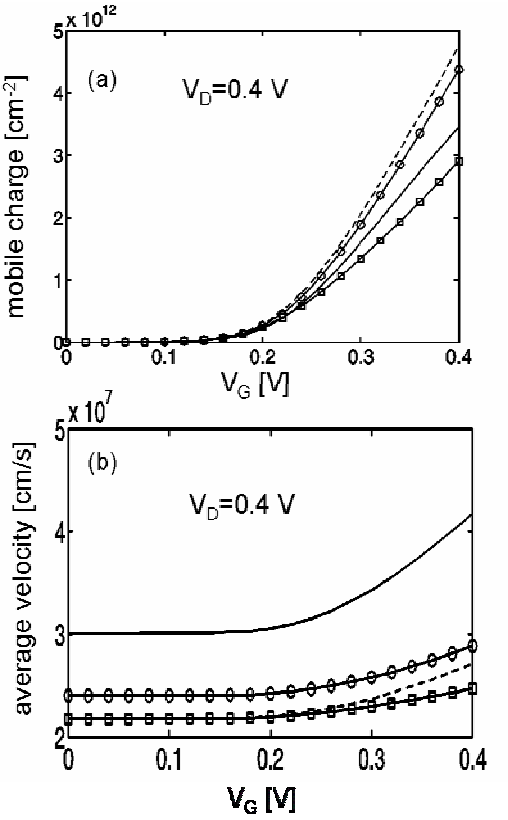

Figure 4: (a) The mobile charge in the channel of the devices vs. V_G at V_{DS}=0.4 V for the four different types of MOSFETs mentioned in Fig. 3(a). (b) The average carrier velocity vs. V_G at V_{DS}=0.4 V for the four types of devices.

Conclusion

In this paper, a theoretical study of electronic structure of armchair carbon nanoribbons compared to zigzag carbon nanotubes using the simple analytical solutions and the numerical solutions is presented. The bandgap of the armchair CNRs is half of that of zigzag CNTs when comparing at equal widths (CNRs) and circumferences (CNTs). Moreover, the degeneracy factor of the lowest subband of armchair CNRs is only one instead of two for zigzag CNTs. This causes the DOS(E) of armchair CNRs to be half of that of zigzag CNTs. In additions, device performance of different types of CNR MOSFETs has been evaluated and compared to a cylindrical gate CNT MOSFET. The study shows that CNR devices can outperform planar Si MOSFETs and provide comparable ON-current densities with CNT MOSFETs, which makes CNR devices a potential candidate for MOSFET devices.

Acknowledgements

The work at national university of Singapore was supported by MOM under grant R-263-000-416-112 and R-263-000-416-133. The work at Purdue University was supported by the Semiconductor Research Corporation (SRC). The Network for Computational Nanotechnology (NCN) computational resources were used.

References

[1] K. S. Novoselov, A. K. Geim, S. V. Morozov, D. Jiang, M. I. Katsnelson, I. V. Grigorieva, S. V. Dubonos, A. A. Firsov, "Two-dimensional gas of massless Dirac fermions in graphene", *Nature*, **438** 197, 2005.

[2] A. Javey, J. Guo, Q. Wang, M. Lundstrom, and H. Dai, "Ballistic carbon nanotube field-effect transistors," *Nature*, vol. **424**, pp. 654-657, Aug 2003.

[3] J. Kong, N. Franklin, C. Chou, S. Pan, K. Cho and H. Dai, "Nanotube molecular wires as chemical sensors," *Science*, vol. **287**, pp. 622-625, Jan 2000.

[4] J. A. Misewich, R. Martel, Ph. Avouris, J. C. Tsang, S. Heinze, and J.Tersoff, "Electrically induced optical emission from a carbon nanotube FET," *Science*, vol. **300**, pp. 783-786, May 2003. J. Chen, V. Perebeinos, M. Freitag, J. Tsang, Q. Fu, J. Liu, and P. Avouris, "Bright infrared emission from electrically induced excitons in carbon nanotubes," *Science*, vol. **310**, pp. 1171-1174, Nov. 2005.

[5] R. Saito, G. Dresselhaus, M. Dresselhaus, *Physical Properties of Carbon Nanotubes*, Imperial College Press, London (1998).

[6] G.-C. Liang, N. Neophytous, D. Nikonov, and M. Lundstrom, "Performance Projections for Ballistic Graphene Nanoribbon Field-Effect Transistors", to appear *IEEE Trans. Electron Devices*, 2007.

[7] B. Obradovic, R. Kotlyar, F. Heinz, P. Matagne, T. Rakshit, D. Nikonov, M. D. Giles, and M. A. Stettler, "Analysis of graphene nanoribbons as a channel material for field-effect transistors," *Appl. Phys. Lett.*, vol. **88**, 142102, Apr. 2006.

[8] K. Wakabayashi, "Electronic transport properties of nanographite ribbon junctions," *Phys. Rev. B*, vol. **64**, 125428, Sep. 2001. K. Nakada, M. Fujita, G. Dresselhaus, M. Dresselhaus, "Edge state in graphene ribbons: Nanometer size effect and edge shape dependence," *Phys. Rev. B.* vol. **54**, 17954, Jun. 1996.

[9] M. Lundstrom and J. Guo, *Nanoscale Transistors: Device Physics, Modeling and Simulation*, Springer (2006).

[10] A. Rahman, J. Guo, S Datta, and M. Lundstrom, "Theory of ballistic nanotransistors,"*IEEE Trans. Electron Devices*, vol. **50**, pp. 1853-1164, Sep. 2003.

[11] S. Datta, *Quantum Transport: Atom to Transistor*, Cambridge (2005).

[12] Y. Ouyang, Y. Yoon, J. Fodor and J. Guo, "Comparison of performance limits for carbon nanoribbon and carbon nanotube transistors", *Applied Physics Letters*, **89** 203107, 2006.